Article

Impact of Wire Geometry in Energy Extraction from Salinity Differences Using Capacitive Technology

Bruno Bastos Sales, Odne S. Burheim, Fei Liu, Olivier Schaetzle, Cees J.N. Buisman, and Hubertus V.M. Hamelers

Environ. Sci. Technol., **Just Accepted Manuscript** • Publication Date (Web): 10 Sep 2012

Impact of Wire Geometry in Energy Extraction from Salinity Differences Using Capacitive Technology

*Bruno B. Sales, [1,2] Odne S. Burheim, [2,3] Fei Liu, [1,2] Olivier Schaetzle, [2] Cees J. N. Buisman[1,2] Hubertus V. M. Hamelers,[1,2]**

[1]Sub-Department of Environmental Technology, Wageningen University, Bornse Weilanden 9, 6708 WG Wageningen, The Netherlands. [2]Wetsus, Centre of Excellence for Sustainable Water Technology, Agora 1, 8932 CJ Leeuwarden, The Netherlands. [3]Department of Chemistry, NTNU - Norwegian University of Science and Technology, N-7491 Trondheim, Norway

*To whom correspondence should be addressed. E-mail: bruno.bastos@wetsus.nl

Footnote: Corresponding Author Phone: +31582843000; Fax: +31582843001; e-mail: bruno.bastos@wetsus.nl; Address: Wetsus, Centre of Excellence for Sustainable Water Technology, Agora 1, 8932 CJ Leeuwarden, The Netherlands.

ABSTRACT: Energy extraction based on Capacitive Donnan Potential (CDP) is a recently suggested technique for sustainable power generation. CDP combines the use of ion-exchange membranes and porous carbon electrodes to convert the Gibbs free energy of mixing sea and river water into electric work. The electrodes geometry has a relevant impact in internal resistance and overall performance in CDP. In this work we present the first effort to use wire shaped electrodes and its suitability for improving CDP designs. Analytical evaluation and electrical measurements confirm a strong non-linear decrease in internal resistance for distances between electrodes smaller than 3 mm. We also demonstrated that we get more power per material invested when compared to traditional flat plate

designs. These findings show the advantages of this design for further development of CDP into a mature technology.

TOC

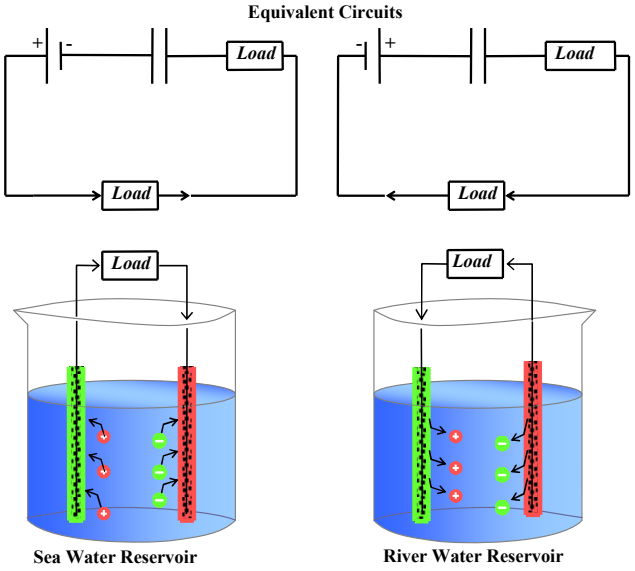

KEYWORDS: Blue Energy; Salinity Difference, Supercapacitors, Wires.

Introduction

The oceans have long been considered a great source of energy available in many different forms [1], but the vast research effort has focused on waves, tidal and offshore wind power [2]. Salinity difference is a frequently overlooked and neglected source of renewable clean energy with a worldwide potential of 2 TW [3]. Yet, this source ranks first place in energy density per water volume and second place in global power potential when compared to all marine renewable power sources [4]. Moreover, salinity difference is a steady source of energy much less sensitive to weather conditions than its concurrent renewable energy sources. The production of electricity with this method is obtained from the free energy available when electrolyte solutions of different concentrations are mixed [5].

Theoretically, in order to harvest energy from salinity gradients, any of the various seawater desalination techniques at present can be modified and the reverse process implemented [6]. Several methods to exploit this potential were proposed and investigated over the last decades [7], with

fundamentally different working principles. Currently the most developed technologies [8, 9] for energy conversion from salinity differences are Pressure Retarded Osmosis (PRO) [10, 11] and Reverse Electrodialysis (RED) [12, 13]. Nevertheless, a need for different and improved techniques remains due to the engineering complexities (design and hydrodynamic challenges) of these systems and their durability when exposed to local environments (e.g. biofouling) [14]. Thus several novel suggestions were reported involving the use of solid-state electrodes [15-19] or nanopores [20] to extract and convert this free energy. In particular, CDP [15, 16] is an electrochemical technique combining the high energy storage and power delivery of porous carbon electrodes [21, 22] with the selectivity of ion-exchange membranes [23]. The driving force of this process is directly related to the membrane equilibrium potential also known as the Donnan Potential [24].

One advantage of this technology, where the repeatedly switch between sea and river water causes the consecutive inversion of electrical potential, is that fouling can be drastically reduced [25] which is a common obstacle in membrane systems. Nevertheless, lowering the ohmic losses is one major issue in all electrochemical techniques [26, 27]. Flow distribution and mass transport issues have also been reported as bottlenecks in this field [28]. In this paper we present a new design using wire shaped electrodes that reduces significantly the ohmic losses. It also allows the design of closed systems with less mechanical resistance (e.g., spacers between membranes) for water flow [29, 30].

The aim of this work is to demonstrate the advantages of cylindrical wires in CDP with an analytical evaluation, the development of a model and experimental validations with electrical and power performance measurements.

Theory

CDP is a two-step cyclic process where we alternate sea and river water between the electrodes. The sea water step consists of ion adsorption on the carbon surface, followed by ion release in the river water step. This ion migration generates a spontaneous electron flow via the external circuit where electricity is extracted. Therefore, our operation method has a constant closed RC circuit joined by the electrodes as the capacitor and an external resistor.

The CDP process is driven by the product of electrochemical potential difference across the compartment containing two membranes covering the carbon electrodes. Figure 1 shows the equivalent electrical circuits of CDP during charge and discharge processes. The Donnan Potential, E_{donnan}, acts as the driving force for ionic current. This potential is spontaneously formed at the membrane surface and changes with the solution concentration. When alternating the immersion of the pair of wires in different salinities, E_{donnan} changes and the electrical double-layer potential, E_{dl}, on the carbon electrodes builds up to attain the opposite potential. The difference between E_{donnan} and E_{dl} is named E_{net} and is the actual driving potential for the energy extraction.

FIGURE 1

The change in adsorbed charge on the capacitive material, C_E, induces a transient current in the external circuit that leads to a voltage drop in the load, R_{ext}. When the equilibrium is reached, there is no electric current anymore and then we immerse the cell in a solution with different concentration to continue the cycle of adsorption/desorption. The voltage and power output of this process are given by

$$E^{cell} = E_{donnan} \cdot \exp\left(-\frac{t}{\tau}\right) \cdot \left(\frac{R_{ext}}{R_i + R_{ext}}\right) \quad (1)$$

$$P^{cell} = \left(E_{net}\right)^2 \cdot \frac{R_{ext}}{\left(R_i + R_{ext}\right)^2} \quad (2)$$

where R_i is the internal resistance of the cell, t is time and τ is the capacitor constant.

Different from traditional supercapacitors, where highly concentrated electrolytes are used [31], the CDP technology in comparison works with much lower conductivities, because it is bound to use sea and, in particular, river water. Therefore the electrolyte resistance is included in the total internal resistance of the cell and corresponds to a large fraction of it. In Equation 2, the dependence of the power output to the ratio of internal and external resistances can be seen. Ideally, for extracting maximum power, R_{ext} should be fixed equal to R_i and R_i should be minimized as much as possible. Aiming to decrease the R_i without compromise to other losses, we propose the use of wire shaped electrodes instead of the usual flat plates design.

For analytical comparison of cell internal resistances between wire and flat plate designs, we focus the study in the region between the two electrodes.

The resistance between electrodes of different shapes can be calculated using mathematical methods described by Vanysek [32]. Considering parallel plates with infinite width, w, and length, L, the resistance between the plates is linear to the electrode intermediate distance, x, as given by [32]

$$R^{\parallel} = \frac{x}{\kappa L 2r}, \text{ for } w = 2r \tag{3}$$

where κ is the solution conductivity.

When comparing with the resistance between two wires, we make the following assumptions: 1. The two electrodes, with radius r, have their centers separated by a distance x (horizontally) and immersed in an infinitely large electrolyte volume; 2. The electrodes are separated in a narrow channel of $2r$ (vertically). The relations are then given by

$$R^{\supset\subset} = \frac{x}{\kappa L 4r}\left(\frac{1}{\sqrt{1-\left(\frac{2r}{x}\right)^2}}\arctan\left[\frac{\left(1-\frac{2r}{x}\right)}{\sqrt{1-\left(\frac{2r}{x}\right)^2}}\right]\right)^{-1} \tag{4}$$

and

$$R^{\supset\subset} = \frac{x}{\kappa L \pi r}, \text{ for } r << x \tag{5}$$

considering the electrodes interdistance. A more detailed explanation for equation 4 can be found in the Appendix A of this manuscript.

Materials and Methods

A pair of inert wires coated with activated carbon and ion selective membranes was alternately dipped in artificial sea and river water in order to deliver electric work. For the theoretical analysis, we modeled the power output as function of the distance between the wire electrodes in a beaker. In this section, we first give the details of the materials and the experimental setup, followed by the details of the applied model.

Electrode preparation.

The porous capacitive electrode solution was made by adding a binder solution to activated carbon (AC). For this, we first dried the AC powder (DLC Super 30, Norit, Amersfoort, The Netherlands) for 24 h in an oven at 105 °*C* to prevent any adsorbed water in the crude sample. The dried carbon was added to a solution of polyvinilidene fluoride (PVDF) (KYNAR HSV 900, Arkema Inc. Philadelphia, USA) in 1-methyl 2-pyrrolidone (NMP). The mixed solution was put into a ball mill grinder (PM 100, Retsch, Haan, Germany) with 12 agate stone balls for 30 minutes at 450 RPM to achieve homogeneous mixing. The slurry was then cast onto metal wires composed of an alloy of titanium and platinum (2 mm thick, Magneto Special Anodes BV, Schiedam, the Netherlands) over a length of 6 cm leaving the extremities free for electrical connections and to neglect fringing of the electric field at the ends. After casting, the wires were put in a vacuum oven at 50 °*C* to let all the NMP evaporate and to achieve a content of 10 w% PVDF in the electrode. The membrane layer was obtained by painting an ionomer solution over the carbon layer. Anionic ionomer (Fumion FAA, Fumatech, St. Ingbert, Germany) was used to make the anode and cationic ionomer (Fumion FLNMP-915, Fumatech, St. Ingbert, Germany) was used to make the cathode. Together both layers added, in average, 120 μm to the wire thickness.

Artifical sea and river water.

Different salt concentration solutions were made to simulate "sea" and "river" water. The set river concentration C_{river} consisted of 1 g NaCl/L, while the sea concentration was 30 g NaCl/L. All solutions were kept in 1 L containers stored in a thermostat (FRIOCELL, MMM Medcenter, Munich, Germany) at 25 °*C* before all experiments.

Setup and measurements.

The experimental setup used in this study consisted in a rectangular frame in which the wires were positioned parallel to each other. The distance between the wires could be precisely set and changed between 29, 19, 9 or 1 mm. The wires were connected via an external circuit counting a resistor (Figure 1).

During the CDP cycle, the setup cell was alternately immersed in sea and river water in large containers, always waiting until the potential reached 0 V before switching to allow a constant flow of ions and electrons. The potential of the setup cell was logged by a precision multimeter (Fluke 8846A 6.5 digit, Everett, USA), and the internal resistance was logged by a high-speed milliohmeter (Agilent 4338A, Santa Clara, USA). This procedure was repeated several times keeping the intermediate distance constant.

Model of Internal Resistance and Power.

We have from equation 5 that the relation between the electrolyte resistance and the distance between the wires, x, is highly non-linear. On the other hand, this analytical expression does neither account for the back side of the wire nor the vast additional electrolyte volume in the container of our experiments. Therefore we modeled the power output for two electrodes of 2.5 mm in a container as a function of x and compared this to the analytical expression and the measured values. We also included different flat plate designs to confirm, in order magnitude consideration, the superiority of wires over plates.

The modeling was done with the Finite Element Mesh (FEM) tool Comsol Multiphysics 2.1. The model was a Faraday one assuming one electrode with an iso-potential equal to the ground whereas the other with iso-potential of 50 mV (half of the maximal experimentally obtained potential). By analyzing the total current in light of the applied potential, the electrolyte resistance and power were obtained. The model was verified by checking that it was mesh size independent.

Results and Discussion

We see several consecutive CDP cycles with regular behavior in Figure 2, with distance between electrodes set to 29 mm and R_{ext} to 60Ω. The CDP cycle starts when immersing a cell with a pair of electrodes, previously equilibrated in river water, into sea water and then returning it to river water to end this adsorption/desorption cycle. Figure 2 is in accordance with equation 1 that describes in the adsorption step, when the cell is immersed in sea water and t = 0 s, the E_{donnan} sets instantly the initial and maximum cell voltage. This autogenerated potential drives ion transport through the membranes and into the nano porous carbon electrodes where they are adsorbed, requiring an external electric current to

keep electroneutrality. Over time, one can observe the cell potential decreasing exponentially with the adsorption of ions on the carbon surface electrical double-layer. This continues until E^{cell} reaches 0 V (system is in equilibrium) and the charging of the nano porous supercapacitor reaches saturation.

FIGURE 2

At the point of equilibrium, the E_{dl} corresponds to E_{donnan} when the membranes are exposed to sea water. We then start the second step of the cycle by switching the cell to river water. Now, the E_{donnan} reverses its sign and the driving force leads to ion desorption. The behavior described in the previous step is also observed here, but with different amplitude of values for E^{cell}. Equations 1 and 2 successfully predict this difference in voltage and potential obtained in each step, due to much higher R_i in river water than in sea water.

FIGURE 3

The higher and more crucial R_i in river water was modeled in different geometries and the results can be seen in Figure 3. The inverse values of x and R_i are plotted in the graphs for convenience, i.e. to emphasize the geometry impact. Also, the positions where we have experimental validation are indicated by dashed rings. In the upper graph we plotted the difference between 3 electrode geometries: wires, double sided plates and one sided plates. One sided plates is the traditional design in supercapacitor technologies, however double sided plates are commonly used when cells are put in parallel [33]. In our experiments, the double sided plates can be seen as an intermediate, or transition, in comparing wires to single sided plates. We include this to demonstrate that there is hardly any contribution from the single/double sided effect and that, again, the advantage is solely due to the cylindrical shape of the electrode. At large distances in the curves, we observe no substantial difference among the modeled designs. In contrast, when the electrodes are positioned closer to each other, the wire shape starts to show its advantage. As expected, we see a linear response of R_i with variation of the distance between plates while a strong non-linear relation is observed for wires, especially in the region of 350 m^{-1}.

Using the assumptions made to derive the analytical expressions shown in equations 3, 4 and 5, we continue the analysis with focus on the difference of R_i between semi-wires and one sided plates (Figure 3). Already here, we can observe the advantage of wires over one sided plates from the 100 m^{-1} distance region.

The actual R_i measured in river water were 73 Ω for 29 mm, 62 Ω for 19 mm, 47 Ω for 9 mm and 10 Ω for 2.6 mm. One can see the agreement between the measured and modeled resistances. As for the analytical expressions, they give a further qualitative view of the difference between the two geometries. They describe, and the actual measured values confirm the model, a trend in this particular situation of two electrodes in a large container.

FIGURE 4

With the cell voltage and the fixed external resistance known, we can calculate the power density (per weight of carbon material) of the whole cycle in this CDP technique. After several cycles logged for each distance set between electrodes, the average power density obtained was 70±5 μW/g for 29 mm, 74±3 μW/g for 19 mm, 163±18 μW/g for 9 mm and 347±12 μW/g for 1 mm. The average value of carbon material per length of wire was 0.85 g/m and it was used in our model to predict the power density for two wire electrodes. Figure 4 shows the experimental confirmation of the expected trend in the model (dashed curve) when wire shaped electrodes are used. The power densities do not vary much at large distance, but once again we see the non-linear behavior of the wires when they are put adjacent to each other. The measured values fit nicely to the theoretical curve, except for x = 9 mm. We assume that other neglected ohmic losses, experimental disturbances when holding the wires and partial immersion of the electrodes respond for this deviation. The graph verifies the analysis of superior overall performance of the system when using wires, not only in lowering ohmic losses, but also allowing a higher power density.

These results present also novel possibilities within salinity gradient technologies. The fact that we are displacing the electrodes, instead of water bodies, opens the door for lowering irreversible losses, e.g.

pumping. One possible design is to make a carrousel of wire electrodes that alternately is immersed in channels where river and sea water are constantly flowing, or batch wise replaced.

Additionally to these advantages, the use of wire shaped electrodes also brings a better ratio of materials used and the electrode-electrolyte surface area. When we consider a fixed volume of activated carbon slurry and ionomer solutions, by applying the same layer thickness of these materials on the designs, we obtain more surface area with the wires. This way we can increase the performance of ion adsorption of the whole process, with the same value of financial investment. Therefore we have another strong argument for applying a wire design in CDP.

This work shows the promising suitability of a wire design for electricity production based on the Capacitive Donnan Potential principle. We observed fundamental differences in the internal resistance dependence to the distance between electrodes when wire shaped electrodes are used instead of flat plate ones. Therefore, the geometry of the electrodes plays an important role in the overall CDP performance.

We have demonstrated that changes in the cell design are a very efficient path for improvement and further development of electrochemical capacitive salinity difference power sources. This was shown analytically and by modeling of the process, in combination with an experimental verification.

In conclusion, with this new geometry of electrodes, it is possible to increase power extraction per mass unit of electrodes, through changes in the cell design, electrode shape and operating condition.

ACKNOWLEDGMENT. Thanks are due to Dhan Prasam Gautam for assistance with the experiments and to Michel Saakes for valuable discussions. This research was performed in the TTIW-cooperation framework of Wetsus, Centre of Excellence for Sustainable Water Technology. Wetsus is funded by the Dutch Ministry of Economic Affairs, the European Union Regional Development Fund, the Province of Friesland, the City of Leeuwarden, and the EZ/Kompas program of the "Samenwerkingsverband Noord-Nederland". We thank the members of the research theme "Blue Energy" in Wetsus for their participation in this research.

Appendix A.

The equation of Resistance

The derivation of equation 4 is done with the assumption that two wires are placed in a slit with insulating walls adjacent to the wires. We chose to solve the integral for the quarter cylindrical symmetry.

$$\frac{1}{R} = \int \kappa \frac{dA}{l}, \text{ where; } dA = rL\, d\phi \tag{A.1}$$

$$\frac{1}{R} = \kappa L \frac{r}{x} \int_0^{\frac{\pi}{2}} \frac{d\phi}{\left(1 - \frac{2r}{x}\cos\phi\right)}, \text{ where; } l = x - r\cos\phi \tag{A.2}$$

solving the integral we obtain:

$$\frac{1}{R} = \frac{\kappa L 2r}{x} \frac{2}{\sqrt{1-\left(\frac{2r}{x}\right)^2}} \arctan\left[\frac{\left(1-\frac{2r}{x}\right)}{\sqrt{1-\left(\frac{2r}{x}\right)^2}}\right], \text{ for } r \le x \tag{A.3}$$

Finally, to compare the geometries when the electrodes are remotely distanced:

$$\frac{1}{R} = \frac{\kappa L \pi r}{2x} \Leftrightarrow R = \frac{2x}{\kappa L \pi r}, \text{ for } r << x \tag{A.4}$$

$$R^{\supset\subset} = \frac{x}{\kappa L \pi r}, \text{ for } r << x \tag{A.5}$$

$$R^{\text{II}} = \frac{x}{\kappa L\, \varpi}, \quad \text{for } r << x \tag{A.6}$$

REFERENCES

1. Isaacs, J. D.; Schmitt, W. R., Ocean Energy: Forms and Prospects. *Science* **1980,** *207*, (4428), 265-273.
2. Gross, R.; Leach, M.; Bauen, A., Progress in renewable energy. *Environment International* **2003,** *29*, (1), 105-122.
3. Post, J. W.; Hamelers, H. V. M.; Buisman, C. J. N., Energy Recovery from Controlled Mixing Salt and Fresh Water with a Reverse Electrodialysis System. *Environmental Science & Technology* **2008,** *42*, (15), 5785-5790.
4. Wick, G. L.; Schmitt, W. R., Prospects For Renewable Energy from the Sea. *Marine Technology Society Journal* **1977,** *11*, (5-6), 16-21.
5. Veerman, J.; Saakes, M.; Metz, S. J.; Harmsen, G. J., Electrical Power from Sea and River Water by Reverse Electrodialysis: A First Step from the Laboratory to a Real Power Plant. *Environmental Science & Technology* **2010,** *44*, (23), 9207-9212.
6. Pattle, R. E., Production of Electric Power by mixing Fresh and Salt Water in the Hydroelectric Pile. *Nature* **1954,** *174*, (4431), 660-660.
7. Jones, A. T.; Finley, W.; Consulting, O. U. S.; San Francisco, C. A. In *Recent development in salinity gradient power*, Oceans 2003. Proceedings, 2003; 2003; pp 2284 - 2287.
8. Boon, N.; van Roij, R., 'Blue energy' from ion adsorption and electrode charging in sea and river water. *Molecular Physics* **2011,** *109*, (7-10), 1229-1241.
9. Ramon, G. Z.; Feinberg, B. J.; Hoek, E. M. V., Membrane-based production of salinity-gradient power. *Energy & Environmental Science* **2011,** *4*, (11).
10. Achilli, A.; Cath, T. Y.; Childress, A. E., Power generation with pressure retarded osmosis: An experimental and theoretical investigation. *Journal of Membrane Science* **2009,** *343*, (1-2), 42-52.
11. Thorsen, T.; Holt, T., The potential for power production from salinity gradients by pressure retarded osmosis. *Journal of Membrane Science* **2009,** *335*, (1-2), 103-110.
12. Burheim, O. S.; Seland, F.; Pharoah, J. G.; Kjelstrup, S., Improved electrode systems for reverse electro-dialysis and electro-dialysis. *Desalination* **2012,** *285*, (0), 147-152.
13. Vermaas, D. A.; Saakes, M.; Nijmeijer, K., Doubled Power Density from Salinity Gradients at Reduced Intermembrane Distance. *Environmental Science & Technology* **2011,** *45*, (16), 7089-7095.
14. Lee, S.; Elimelech, M., Salt cleaning of organic-fouled reverse osmosis membranes. *Water Research* **2007,** *41*, (5), 1134-1142.
15. Sales, B. B.; Saakes, M.; Post, J. W.; Buisman, C. J. N.; Biesheuvel, P. M.; Hamelers, H. V. M., Direct Power Production from a Water Salinity Difference in a Membrane-Modified Supercapacitor Flow Cell. *Environmental Science & Technology* **2010,** *44*, (14), 5661-5665.
16. Liu, F.; Schaetzle, O.; Sales, B. B.; Saakes, M.; Buisman, C. J. N.; Hamelers, H. V. M., Effect of additional charging and current density on the performance of Capacitive energy extraction based on Donnan Potential. *Energy & Environmental Science* **2012,** *5*, (9), 8642-8650.
17. Brogioli, D.; Zhao, R.; Biesheuvel, P. M., A prototype cell for extracting energy from a water salinity difference by means of double layer expansion in nanoporous carbon electrodes. *Energy & Environmental Science* **2011,** *4*, (3), 772-777.
18. La Mantia, F.; Pasta, M.; Deshazer, H. D.; Logan, B. E.; Cui, Y., Batteries for Efficient Energy Extraction from a Water Salinity Difference. *Nano Letters* **2011,** *11*, (4), 1810-1813.
19. Pasta, M.; Wessells, C. D.; Cui, Y.; La Mantia, F., A Desalination Battery. *Nano Letters* **2012**.
20. Guo, W.; Cao, L.; Xia, J.; Nie, F.-Q.; Ma, W.; Xue, J.; Song, Y.; Zhu, D.; Wang, Y.; Jiang, L., Energy Harvesting with Single-Ion-Selective Nanopores: A Concentration-Gradient-Driven Nanofluidic Power Source. *Advanced Functional Materials* **2010,** *20*, (8), 1339-1344.
21. Simon, P.; Gogotsi, Y., Charge storage mechanism in nanoporous carbons and its consequence for electrical double layer capacitors. *Philosophical Transactions of the Royal Society A: Mathematical, Physical and Engineering Sciences* **2010,** *368*, (1923), 3457-3467.

22. Porada, S.; Weinstein, L.; Dash, R.; van der Wal, A.; Bryjak, M.; Gogotsi, Y.; Biesheuvel, P. M., Water Desalination Using Capacitive Deionization with Microporous Carbon Electrodes. *ACS Applied Materials & Interfaces* **2012**.
23. Pivonka, P.; Smith, D.; Gardiner, B., Investigation of Donnan equilibrium in charged porous materials—a scale transition analysis. *Transport in Porous Media* **2007,** *69*, (2), 215-237.
24. Sarkar, S.; SenGupta, A. K.; Prakash, P., The Donnan Membrane Principle: Opportunities for Sustainable Engineered Processes and Materials. *Environmental Science & Technology* **2010,** *44*, (4), 1161-1166.
25. Kerwick, M. I.; Reddy, S. M.; Chamberlain, A. H. L.; Holt, D. M., Electrochemical disinfection, an environmentally acceptable method of drinking water disinfection? *Electrochimica Acta* **2005,** *50*, (25–26), 5270-5277.
26. Lacey, R. E., Energy by reverse electrodialysis. *Ocean Engineering* **1980,** *7*, (1), 1-47.
27. Veerman, J.; Post, J. W.; Saakes, M.; Metz, S. J.; Harmsen, G. J., Reducing power losses caused by ionic shortcut currents in reverse electrodialysis stacks by a validated model. *Journal of Membrane Science* **2008,** *310*, (1-2), 418-430.
28. Vermaas, D. A.; Saakes, M.; Nijmeijer, K., Power generation using profiled membranes in reverse electrodialysis. *Journal of membrane science* **2011,** *385–386*, (0), 234-242.
29. Burheim, O. S.; Liu, F.; Sales, B. B.; Schaetzle, O.; Buisman, C. J. N.; Hamelers, H. V. M., Faster Time Response by the Use of Wire Electrodes in Capacitive Salinity Gradient Energy Systems. *The Journal of Physical Chemistry C* **2012**.
30. Porada, S.; Sales, B. B.; Hamelers, H. V. M.; Biesheuvel, P. M., Water Desalination with Wires. *The Journal of Physical Chemistry Letters* **2012,** *3*, (12), 1613-1618.
31. Stoller, M. D.; Ruoff, R. S., Best practice methods for determining an electrode material's performance for ultracapacitors. *Energy & Environmental Science* **2010,** *3*, (9), 1294-1301.
32. Vanýsek, P., Impact of electrode geometry, depth of immersion, and size on impedance measurements. *Canadian Journal of Chemistry* **1997,** *75*, (11), 1635-1642.
33. Zhao, R.; Biesheuvel, P. M.; Miedema, H.; Bruning, H.; van der Wal, A., Charge Efficiency: A Functional Tool to Probe the Double-Layer Structure Inside of Porous Electrodes and Application in the Modeling of Capacitive Deionization. *The Journal of Physical Chemistry Letters* **2009,** *1*, (1), 205-210.

FIGURE CAPTIONS:

Figure 1: Setup schematics and correspondent equivalent circuit.

Figure 2: Evolution of measured cell potential (mV) over time (s).

Figure 3: Inverse of internal resistance (S) over inverse of electrodes interdistance (m^{-1}) for both wire and plate geometries.

Figure 4: Power densities (μW/g) over electrodes interdistance (mm) for both modeled and measured values using wires.

Figure 1

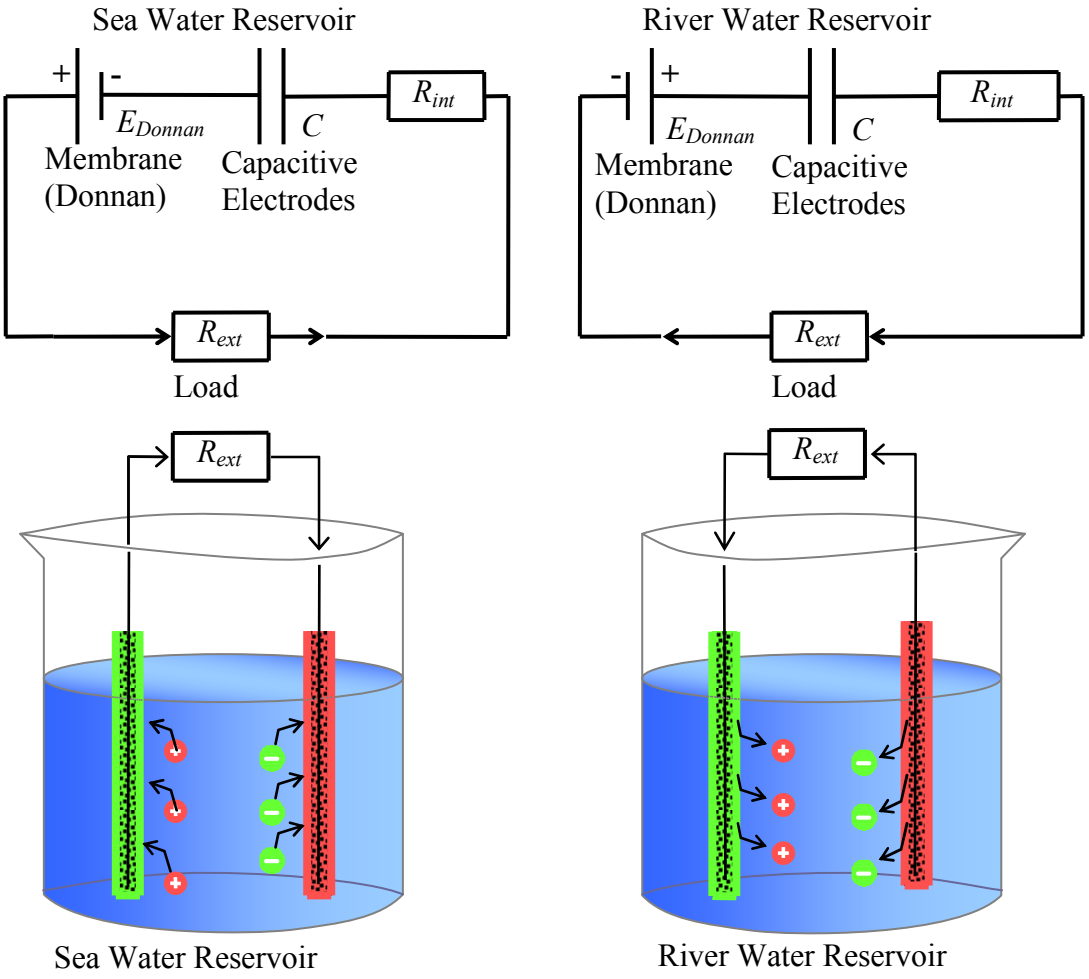
Sea Water Reservoir
+
-
E_{Donnan}
Membrane
(Donnan)
C
Capacitive
Electrodes
R_{int}
R_{ext}
Load
River Water Reservoir
-
+
E_{Donnan}
Membrane
(Donnan)
C
Capacitive
Electrodes
R_{int}
R_{ext}
Load
R_{ext}
Sea Water Reservoir
R_{ext}
River Water Reservoir

Figure 2

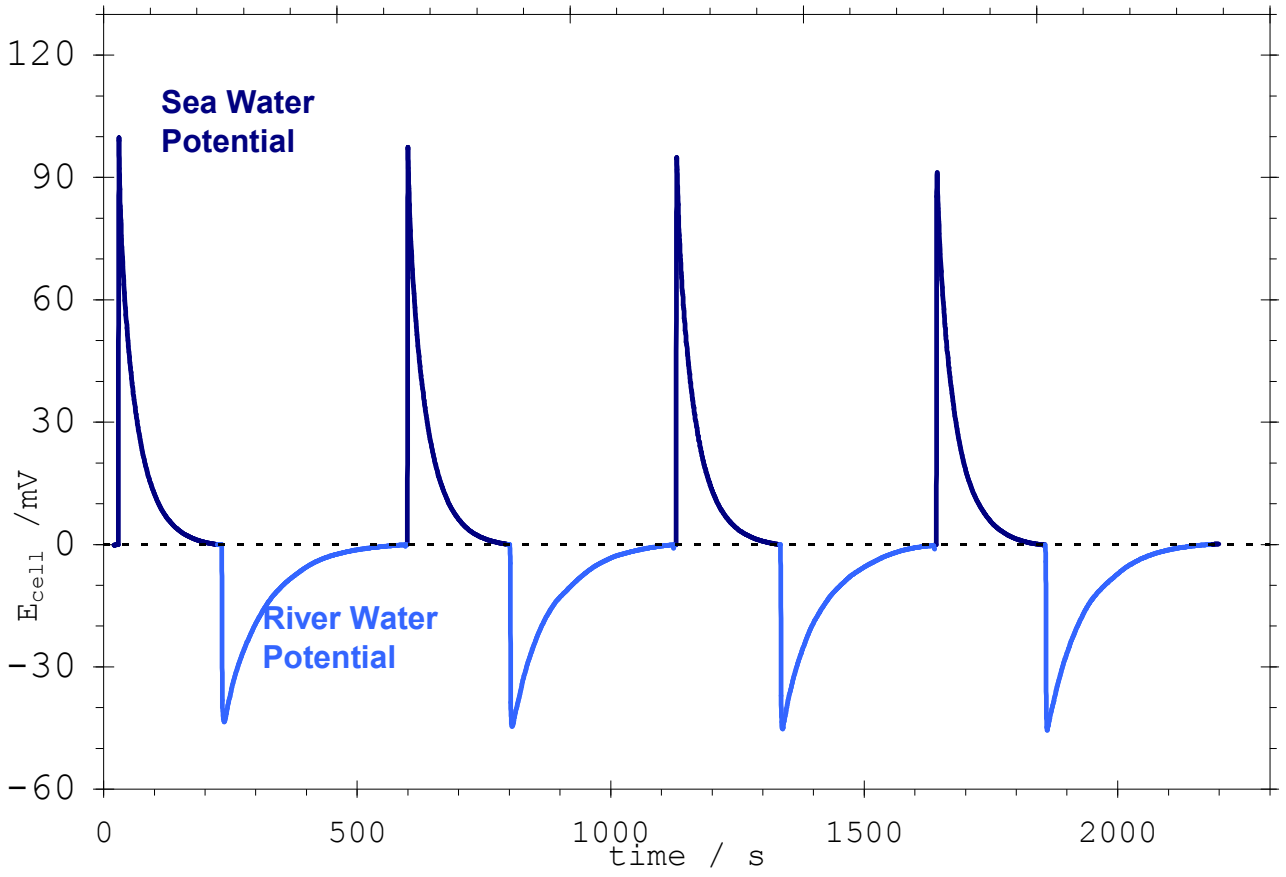
120
90
60
30
0
−30
−60
E_{cell} /mV
Sea Water Potential
River Water Potential
0
500
1000
1500
2000
time / s

Figure 3

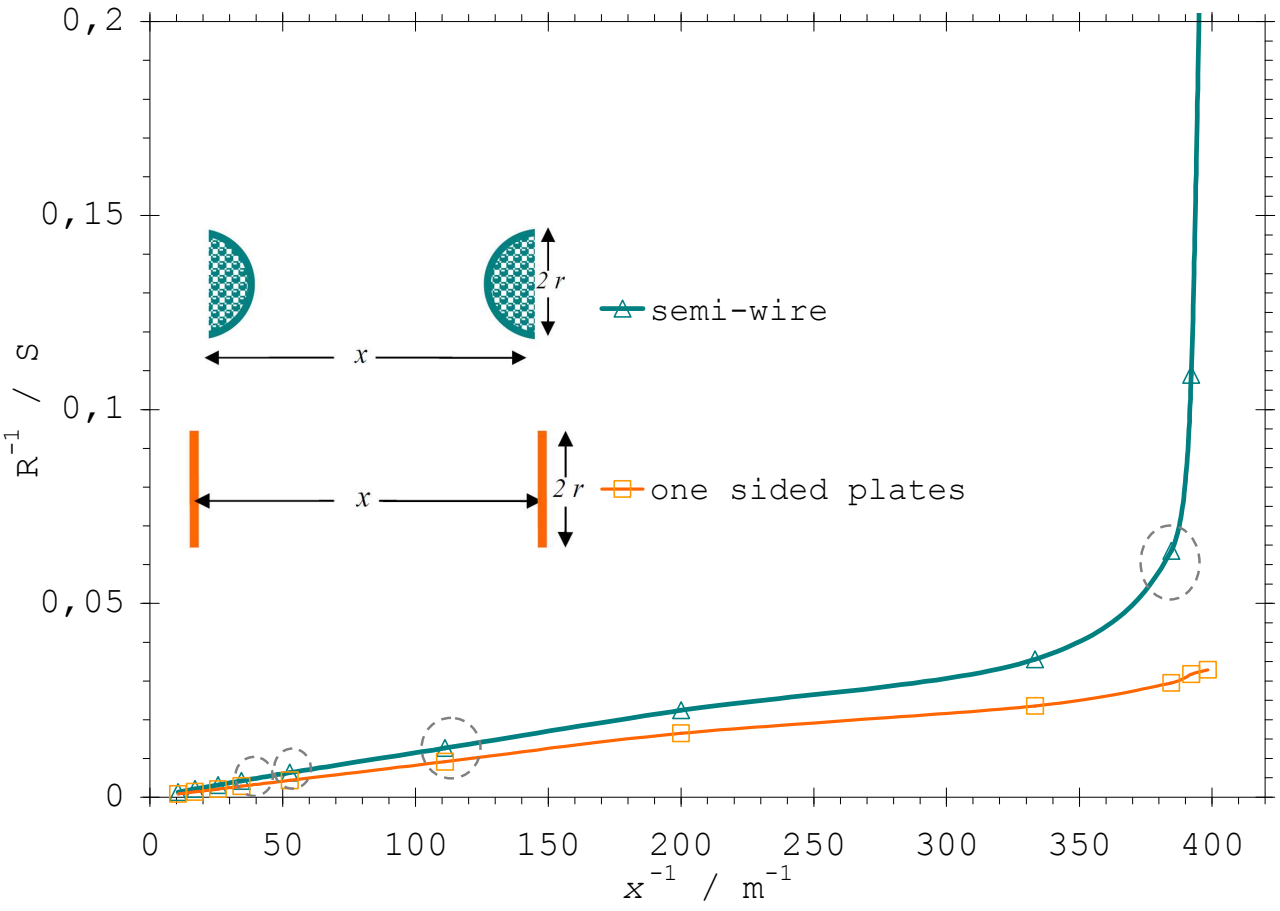
0,2
0,15
0,1
0,05
0
R^-1 / S
0
50
100
150
200
250
300
350
400
x^-1 / m^-1
x
2 r
semi-wire
x
2 r
one sided plates

Figure 4

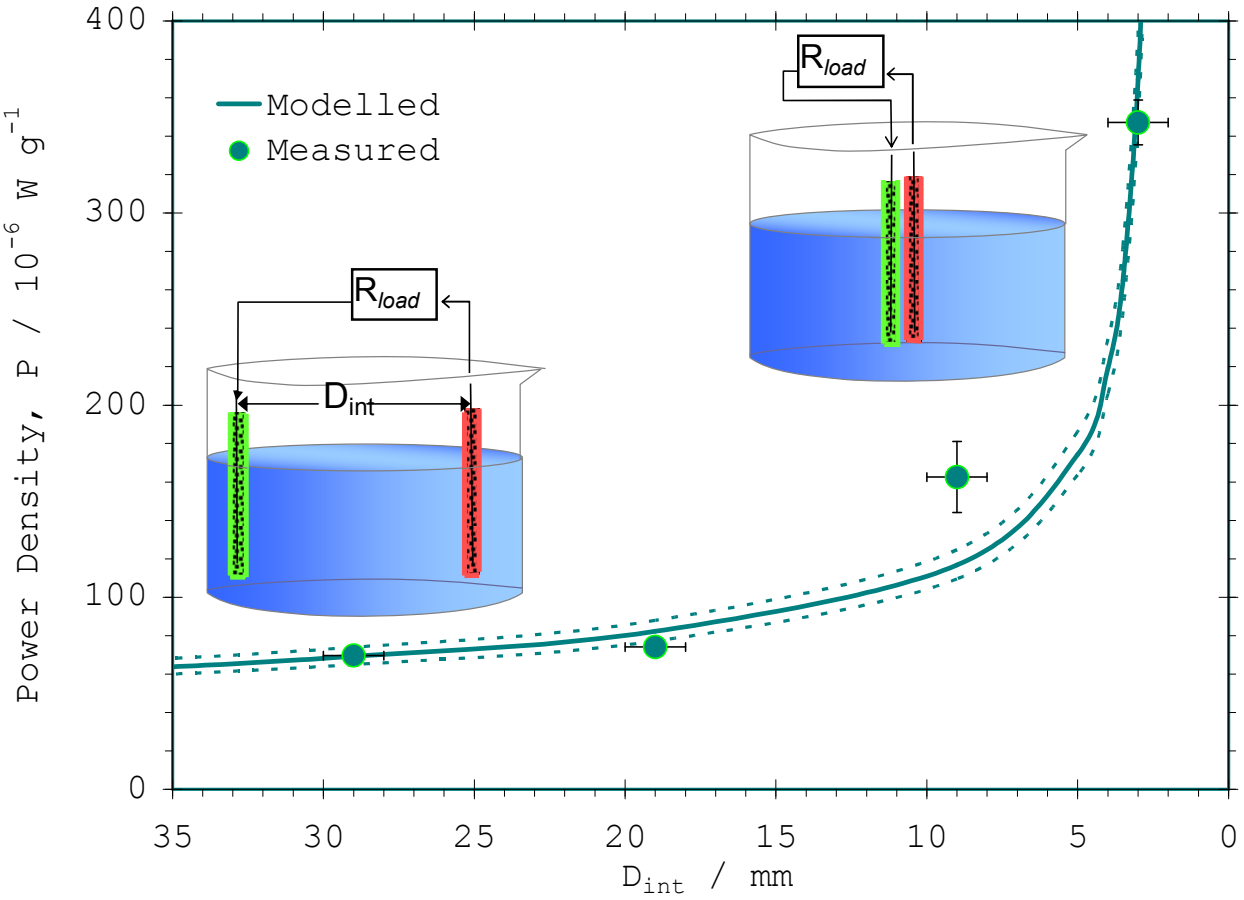
Modelled
Measured
R_{load}
R_{load}
D_{int}
Power Density, P / 10^{-6} W g^{-1}
400
300
200
100
0
35
30
25
20
15
10
5
0
D_{int} / mm